The Knee 26 (2019) 612–618

Contents lists available at ScienceDirect

The Knee

Tibial insertion of the anterior cruciate ligament and anterior horn of the lateral meniscus share the lateral slope of the medial intercondylar ridge: A computed tomography study in a young, healthy population

Yasukazu Yonetani [a,*], Masashi Kusano [d], Akira Tsujii [a], Kazutaka Kinugasa [b], Masayuki Hamada [a], Konsei Shino [c]

[a] Department of Orthopaedic Surgery, Hoshigaoka Medical Center, Osaka, Japan
[b] Department of Orthopaedic Surgery, Osaka Rousai Hospital, Osaka, Japan
[c] Department of Orthopaedic Surgery, Yukioka Hospital, Osaka, Japan
[d] Department of Orthopaedic Surgery, Kansai Rosai Hospital, 3-1-69, Inabaso, Amagasaki, Hyogo 660-0064, Japan

ARTICLE INFO

Article history:
Received 20 November 2018
Received in revised form 7 March 2019
Accepted 9 April 2019

Keywords:
Anterior cruciate ligament
Anterior horn of lateral meniscus
Computed tomography
Bony landmarks
Individual difference
Tibial insertion

ABSTRACT

Background: The central intercondylar ridge (CIR) is an anatomical bony landmark that bisects the slope of the medial intercondylar ridge (MIR) between the tibial insertion of the anterior cruciate ligament (ACL) and anterior horn of lateral meniscus (AHLM) and was recently revealed by computed tomography (CT) evaluation corresponding to histologic slices of cadaveric knees. The purpose of this study was to clarify the shape and size of ACL and AHLM tibial insertion in young, healthy knees using the new bony landmark (CIR) and previously reported landmarks.

Methods: The contralateral healthy knees in 34 ACL-reconstructed patients (18 male patients, 16 female patients, mean age: 24.0 years) were scanned by CT. In the reconstructed coronal/sagittal images, bony landmarks of ACL (anterior: anterior ridge, posterior: blood vessel in tubercle fossa, medial: MIR, lateral: CIR) and AHLM (medial: CIR, lateral: bottom of the slope) were plotted for evaluation. The length of sagittal slices and the width in five coronal slices of the insertion were measured.

Results: The ACL insertion consistently showed a boot-like-shape adjacent to the square shape of AHLM on three-dimensional imaging. The mean ACL sagittal length was 14.5 ± 1.9 mm, while the mean ACL widths (in mm) from anterior to posterior were 12.7 ± 2.7, 8.1 ± 1.9, 7.9 ± 2.0, 7.5 ± 1.5, and 7.2 ± 1.6, which was highly correlated with the tibial plateau size.

Conclusions: The boot-like-shape of the ACL tibial footprint insertion shared the slope of MIR with the rectangular shape of AHLM in young, healthy knees. This study may provide useful information for safe tibial tunnel creation at the time of ACL reconstruction.

1. Introduction

Inaccurate tibial tunnel creation during anterior cruciate ligament (ACL) reconstruction sometimes causes damage to the anterior horn of the lateral meniscus (AHLM) [1–3], as well as inadequate restoration of knee biomechanics. When intraoperatively creating the accurate tibial tunnel, anatomical bony landmarks adjacent to the ACL tibial insertion, which have been

* Corresponding author at: Department of Orthopaedic Surgery, Hoshigaoka Medical Center, 4-8-1 Hoshigaoka, Hirakata City, Osaka 573-8511, Japan.
E-mail address: yonechan-osk@umin.ac.jp. (Y. Yonetani).

https://doi.org/10.1016/j.knee.2019.04.009
0968-0160/

revealed by macroscopic observation, histology, or radiographic evaluation, are widely used. These are the anterior ridge (AR) [4–6] (Figure 1, asterisk), the medial intercondylar ridge (MIR) [6–8] (Figure 1, black arrowhead), and the vessels in the tubercle fossa or the posterior edge of the lateral meniscus [6,8] (Figure 1, red circle). Intraoperatively, these three borders (of four) of the insertion area were well recognized as clear bony contours. However, the lateral border was not macroscopically identified because AHLM and ACL were observed as overlapping structures on the bony surface and complex structures blended together on imaging [9].

Our recent study using elderly cadaveric knees demonstrated the positional relationship between ACL and AHLM tibial insertions, as the histological slices parallel to the fiber arrangement around the AHLM made it possible to distinguish the fibers between the ACL and AHLM [6]. With evaluation using synchronized microscopy and computed tomography (CT), the central intercondylar ridge (CIR) on the slope of the MIR was defined as a new anatomical bony landmark bisecting the slope between the ACL and AHLM tibial insertion (Figure 1, white circle) [6]. Using this recently found bony landmark (CIR) and the previously reported three landmarks, the ACL tibial insertion could be delineated on the tibial plateau using CT imaging.

The purpose of this study was to clarify the shape and size of the ACL and the AHLM tibial insertion of healthy knees in a young population.

2. Methods

2.1. Patients

The contralateral healthy knees in 34 ACL-reconstructed patients (18 males 16 females, mean age: 24.0 ± 8.2 years, mean height: 169.0 ± 8.3 cm, mean weight: 67.3 ± 12.4 kg) (± means Standard deviation) were scanned using CT imaging (Toshiba, Tokyo, Japan). The patient characteristics are presented in Table 1. Ethical approval for this study was obtained from the Hoshigaoka Medical Center Ethical Committee (protocol No.1646).

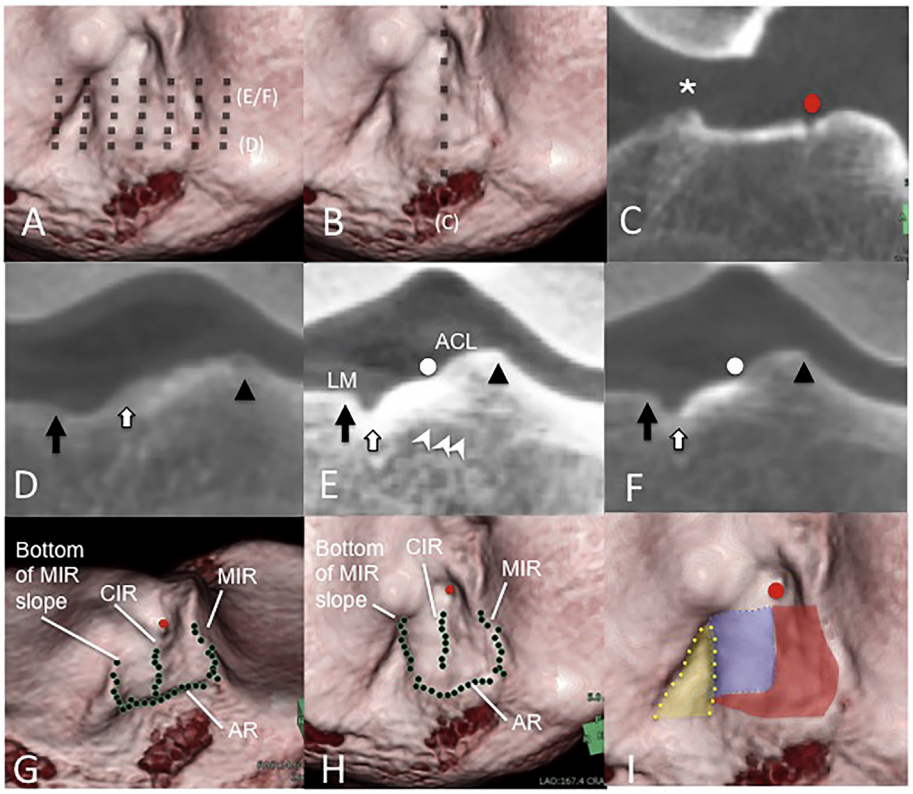

Figure 1. The width of anterior cruciate ligament (ACL) and anterior horn of the lateral meniscus (AHLM) insertion was measured in five coronal slices divided from the anterior and posterior edges of the ACL insertion. (a) Bird's-eye view of the tibial surface with position of coronal view (dotted lines). (b) Bird's-eye view of the tibia with the position of sagittal slice. (c) Sagittal view of ACL insertion: anterior ridge (asterisk), vessel in the tubercle fossa (red dot). (d) Slice 1: anterior margin of ACL. (e) Slice 3: central position in soft tissue window setting. (f) In-bone window setting: medial intercondylar ridge (MIR) (black arrowhead), central intercondylar ridge (CIR) (white circle), bottom of MIR slope (white arrow), trabecular parallel to lateral meniscus (LM) fibers (white arrowhead), lateral intercondylar ridge (black arrow). (g) Anterior view and (h) bird's-eye view of plotted bony landmarks of ACL and AHLM (green dots). (i) Scheme of insertion. Shape of ACL (red area) was 'boot-like' adjacent to AHLM (blue area). 'Lateral groove' (yellow area).

Table 1
Demographic data.

n = 34	Mean ± SD	Range
Age	24.0 ± 8.2 years	15–46
Height	169.0 ± 8.4 cm	152–183
Weight	67.3 ± 12.4 kg	50–93
Antero-posterior diameter of tibial plateau	50.5 ± 4.6 mm	43.0–58.9
Transverse diameter of tibial plateau	74.5 ± 6.9 mm	64.2–86.8

SD, standard deviation.

2.2. Plotted bony landmarks on CT images

Coronal slices, which were parallel to the posterior line of the tibial plateau (Figure 1(a,d–f)), and sagittal slices, which were perpendicular to coronal slices (Figure 1(b,c)), were simultaneously reconstructed every one millimeter using software (SYNAPSE VINCENT, FujiColorFilm, Tokyo, Japan). The bony landmarks of the ACL and AHLM tibial insertion were plotted on the coronal and sagittal CT images in both bone (Figure 1(c,d,f)) and soft tissue windows (Figure 1(e)). The landmarks of ACL tibial insertion were used as follows: anterior edge, anterior ridge (Figure 1(c), asterisk); posterior edge, blood vessel in the tubercle fossa (Figure 1(c,i), red circle); medial edge, MIR (Figure 1(d–f), black arrowhead); and lateral edge, CIR (Figure 1(e,f), white circle). Also, the landmark of the AHLM tibial insertion was used as the lateral edge, bottom of the MIR slope (Figure 1(d–f), white arrow); and medial edge, CIR (Figure 1(e,f), white circle). The landmark of 'lateral groove' was used as medial edge, bottom of MIR slope (Figure 1(d–f), white arrow); and medial edge, lateral intercondylar ridge (Figure 1(d–f), black arrow). When plotting these landmarks, characteristic findings around the ACL and AHLM tibial insertion were used, as follows. The cortex of the ACL tibial insertion was concave in coronal images (Figure 1(f)). The cortex of the AHLM was convex and thickened (Figure 1(f)), and the trabecular tissue beneath the insertion was parallel to the AHLM fibers in coronal images (Figure 1(e), white arrowhead).

2.3. Measuring length and width of ACL and AHLM tibial insertion

The sagittal length of the ACL tibial insertion was measured in the reconstructed sagittal slice, which included AR and vessels in the tubercle fossa (Figure 1(c)). Coronal widths of the ACL and AHLM tibial insertion were measured in five coronal slices, which were divided into the anterior and posterior edge of the ACL tibial insertion (slice number defined from anterior to posterior) (Figure 1(a,d–f)). The ratio of ACL insertion to slope of MIR was calculated in each coronal slice. The shape of the slope of the MIR, ACL and AHLM tibial insertion was evaluated by recognizing each plotted area on the reconstructed three-dimensional (3D) image when viewed from above (bird's-eye view) (Figure 1(h,i); Supplementary data S1).

To scrutinize size variation of the ACL tibial insertion, the following individual information was evaluated: height, weight, antero-posterior and transverse diameter of the tibial plateau measured in reconstructed CT images (Tables 2, 3; Supplementary data S3, S4).

2.4. Statistical analyses

To evaluate the relationship between the size of the ACL and the size of the AHLM tibial insertion and the relationship between each size of the insertion and physical characteristics of the patient (height, weight, size of tibial plateau), Pearson

Table 2
Results of the correlation between demographic data and the size of anterior cruciate ligament/anterior horn of lateral meniscus tibial insertion (all subjects).

All subjects		Height	Weight	Tibial plateau		ACL sagittal length	ACL width					AHLM width			
				AP	Trans.		Slice 1	Slice 2	Slice 3	Slice 4	Slice 5	Slice 2	Slice 3	Slice 4	Slice 5
Height		1													
Weight		0.76**	1												
Tibial plateau	AP	0.86**	0.85**	1											
	Trans.	0.84**	0.88**	0.96**	1										
ACL sagittal length		0.38*	0.47**	0.38*	0.41*	1									
ACL width	Slice 1	0.51**	0.47**	0.61**	0.55**	0.12	1								
	Slice 2	0.55**	0.63**	0.70**	0.71**	0.28	0.67**	1							
	Slice 3	0.55**	0.62**	0.68**	0.73**	0.25	0.62**	0.81**	1						
	Slice 4	0.52**	0.65**	0.63**	0.68**	0.31	0.57**	0.72**	0.85**	1					
	Slice 5	0.53**	0.54**	0.56**	0.61**	0.33	0.45**	0.52**	0.69**	0.79**	1				
AHLM width	Slice 2	0.41*	0.43*	0.40*	0.43*	0.27	0.44*	0.10	0.21	0.35*	0.26	1			
	Slice 3	0.33	0.30	0.15	0.18	0.25	0.17	0.03	0.01	0.18	0.20	0.57**	1		
	Slice 4	0.44**	0.22	0.34*	0.37*	0.21	0.36*	0.28	0.38*	0.27	0.42*	0.40*	0.60**	1	
	Slice 5	0.32	0.24	0.35*	0.36*	0.26	0.46**	0.35*	0.37*	0.25	0.11	0.59**	0.32	0.60**	1

ACL, anterior cruciate ligament; AHLM, anterior horn of lateral meniscus; AP, antero-posterior diameter; Trans, transverse diameter.
** $P < 0.01$.
* $P < 0.05$.

Table 3
Results of the correlation between demographic data and the size of anterior cruciate ligament/anterior horn of lateral meniscus tibial insertion (separated by male and female subjects).

		Male				Female			
		Height	Weight	Tibial plateau		Height	Weight	Tibial plateau	
				AP	Trans.			AP	Trans.
Height		1				1			
Weight		0.04	1			0.55*	1		
Tibial plateau	AP	0.33	0.23	1		0.66**	0.83**	1	
	Trans.	0.27	0.44	0.81**	1	0.51*	0.74**	0.81**	1
ACL sagittal length		−0.18	0.30	−0.01	−0.03	0.30	0.01	−0.06	0.14
ACL width	Slice 1	0.28	0.06	0.60**	0.45	0.13	0.31	0.21	0.09
	Slice 2	0.20	0.48*	0.75**	0.76**	−0.25	−0.28	−0.23	−0.22
	Slice 3	0.19	0.51*	0.71**	0.77**	0.04	−0.07	−0.01	0.23
	Slice 4	−0.12	0.51*	0.37	0.42	0.09	0.09	0.07	0.29
	Slice 5	0.23	0.30	0.44	0.42	0.31	0.22	0.16	0.49
AHLM width	Slice 2	−0.08	−0.05	−0.23	−0.12	0.21	0.35	0.29	0.30
	Slice 3	0.32	0.15	−0.21	−0.15	0.03	0.24	−0.02	−0.01
	Slice 4	0.55*	−0.03	0.37	0.28	−0.16	−0.31	−0.38	−0.07
	Slice 5	0.17	−0.07	0.20	0.11	−0.53*	−0.54*	−0.47	−0.29

ACL, anterior cruciate ligament; AHLM, anterior horn of lateral meniscus; AP, antero-posterior diameter; Trans., transverse diameter.
** $P < 0.01$.
* $P < 0.05$.

correlation coefficients and the correlation coefficient (R) were calculated. To compare male and female insertion measurements, Student's t-test was used. The significance level was set at $P < 0.05$. For the statistical analyses, we used IBM® SPSS®Statistics 21.0 (Mac® client version, IBM, Armonk, NY, USA).

3. Results

3.1. Characteristic findings of the ACL and AHLM tibial insertion on reconstructed CT slices

All tibial ACL and AHLM bony landmarks were clearly identified in all 34 knees. In the coronal images, the insertion of the ACL was concave, while the insertion of AHLM was convex, with a thick cortex and trabecular tissue parallel to ACL and AHLM fibers in soft tissue and bone window CT images (Figure 1(f)). CIR was located almost centrally on the square shape on the slope of MIR, which was anterior to posterior in all knees (Figure 1(e,f)), except for the anterior portion that was just behind the anterior edge (Figure 1(d)).

3.2. Shape and size of ACL and AHLM tibial insertion

The mean sagittal length of the ACL tibial insertion was 14.5 mm (standard deviation (SD) 1.9). The mean widths of the ACL tibial insertion were 12.7 mm in slice 1 (SD 2.7), 8.1 mm in slice 2 (SD 1.9), 7.9 mm in slice 3 (SD 2.0), 7.5 mm in slice 4 (SD 1.5), and 7.2 mm in slice 5 (SD 1.6) (Figure 2(a)). ACL sagittal length was significantly longer than every ACL width, and the ACL width in slice 1 was significantly longer than ACL widths in remaining slices; there were no significant differences among ACL widths except slice 1 (Figure 2(a); Supplementary data S2). These data verified the boot-like shape of the ACL tibial insertion in the bird's-eye 3D CT view (Figure 1(h,i); Supplementary data S1).

The mean width of the AHLM tibial insertion was 6.8 mm in slice 2 (SD 1.5), 6.7 mm in slice 3 (SD 1.9), 7.1 mm in slice 4 (SD 1.5), and 6.8 mm in slice 5 (SD 2.7). There were no significant differences between the widths of AHLM (Figure 2(b); Supplementary data S2). These data also verified the box shape of the AHLM tibial insertion, which was surrounded by the boot-like shape of the ACL tibial insertion within the square shape of the MIR slope (Figure 1(h,i); Supplementary data S1).

The ACL and AHLM tibial insertion almost equally shared the slope of MIR (Figure 1(e–i)). This is demonstrated by the mean ratios of ACL insertion in the slope of MIR, which were as follows: 57% (SD 10) in slice 2, 53% (SD 7.8) in slice 3, 51% (SD 5.9) in slice 4, and 51% (SD 7.0) in slice 5 (Supplementary data S2). Furthermore, the MIR slope showed stair-step-like undulation on coronal slices (Figure 1(e,f)) and on the front view of 3D imaging (Figure 1(g)).

3.3. Correlation between demographic data and size of ACL and AHLM tibial insertion

The widths of the ACL tibial insertion in slices 2 and 3 were correlated with the transverse diameter of the tibial plateau ($R = 0.71$, 0.73), the antero-posterior diameter of the tibial plateau ($R = 0.70$, 0.68), height ($R = 0.55$, 0.55), and weight ($R = 0.63$, 0.62) (Table 2).

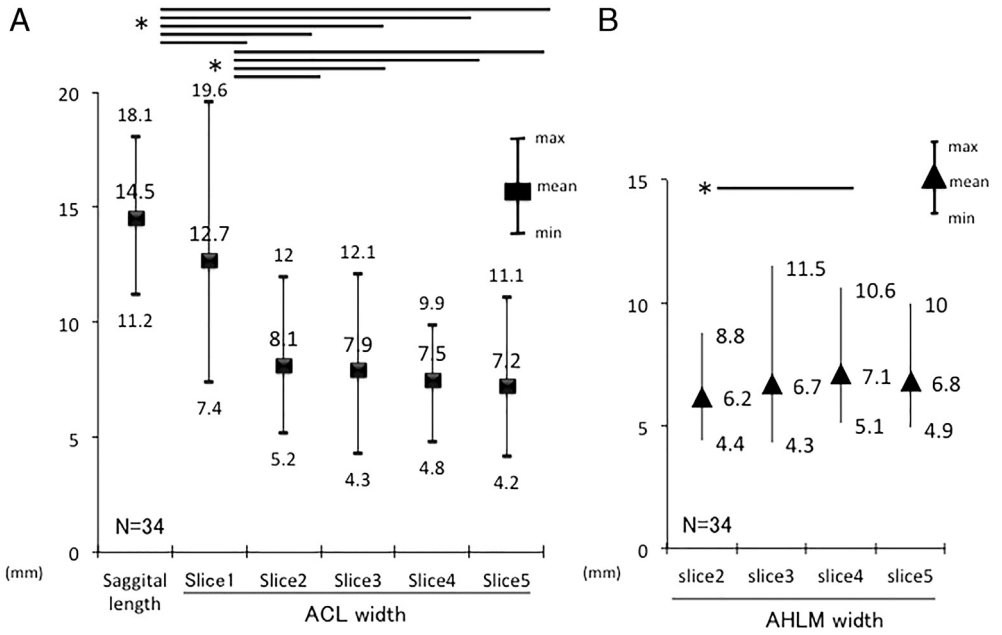

Figure 2. Size of the tibial insertion in (a) anterior cruciate ligament (ACL), and (b) anterior horn of the lateral meniscus (AHLM) (*$P < 0.05$).

Additionally, widths of the AHLM tibial insertion showed a strong correlation for each slice (Table 2; Supplementary data S3, S4). However, the size of the female ACL tibial insertion did not correlate with individual body size, while that of males did correlate with individual body size (Table 3).

4. Discussion

In the present study, the shapes and sizes of the ACL tibial insertion in healthy knees were investigated using the bony landmarks on the coronal, sagittal and reconstructed 3-D CT images using the AHLM tibial insertion as a reference.

Many studies have pointed out individual differences, as well as differences in modality, age, sex, race, and body type, due to a variety of tissue preparations [10]. However, variability in individual interpretations of the examiner with regard to the bony landmarks of tibial insertions on CT imaging was eliminated in this study. The recently found bony landmark CIR, which lengthwise bisects the slope of MIR between the ACL and AHLM tibial insertions, consistently showed a boot-like shape of the ACL tibial insertion around the rectangular shape of the AHLM tibial insertion (Figure 1(i); Supplementary data S1). The width of the mid-portion of the ACL tibial insertion was proportional to individual body size (Table 2).

While previous studies investigated the ACL tibial insertion by macroscopic observation in cadaveric knees [8,9,11–15], few consistent findings were obtained because of various techniques used to dissect the fibrous, synovial, and fat tissues surrounding the ligament [10]. A recent study using three Tesla (3 T) magnetic resonance imaging (MRI) analyzed the tibial insertions by distinguishing ACL and AHLM fibers based on appearance, and showed markedly different results [16]. These discrepancies could be attributed to the differences in the way of defining essential components of the ligament. While the true bone–ligament/tendon interface termed 'enthesis' is observed only by histologic evaluation [17], some histologic examination parallel to ligament fibers using magnified specimens of the small area may lack the positional information of the insertion on the tibial plateau. In addition, there has been no well-designed study to distinguish ACL and AHLM fibers histologically because AHLM and ACL were observed as overlapped structures or complex structures blending together [9]. Our recent study, which used the knees of elderly female cadavers, demonstrated the positional relationship between the ACL and AHLM tibial insertions, as the histological slices parallel to the fiber arrangement around the AHLM made it possible to distinguish the fibers between the ACL and AHLM [6]. With synchronized microscopic and CT evaluation, the CIR on the slope of MIR was defined as the new anatomical bony landmark bisecting the slope between ACL and AHLM tibial insertions [6] (Figure 1(e–h); Supplementary data S1). Considering this recently found bony landmark CIR and the previously reported landmarks together, the current study confirmed that the ACL and AHLM tibial insertions could be delineated on 3-D CT images of the tibial plateau in the young population. This information might be useful for pre-operative planning and postoperative evaluation using CT images or for reducing the risk of damaging the AHLM insertion during the creation of a tibial tunnel for ACL reconstruction [1–3] (Supplementary data S5).

Although all knees were from an Asian population, individual differences in the width of the ACL, which were influenced by height, weight, and antero-posterior and transverse diameter of the tibial plateau, were determined (Table 2). Interestingly, the size of the ACL tibial insertion did not correlate with individual body size in females, while the size of the ACL tibial insertion correlated with the size of tibial plateau and not with height or weight in males (Table 3). These differences among the sexes may somewhat be correlated with the incidence of ACL injuries.

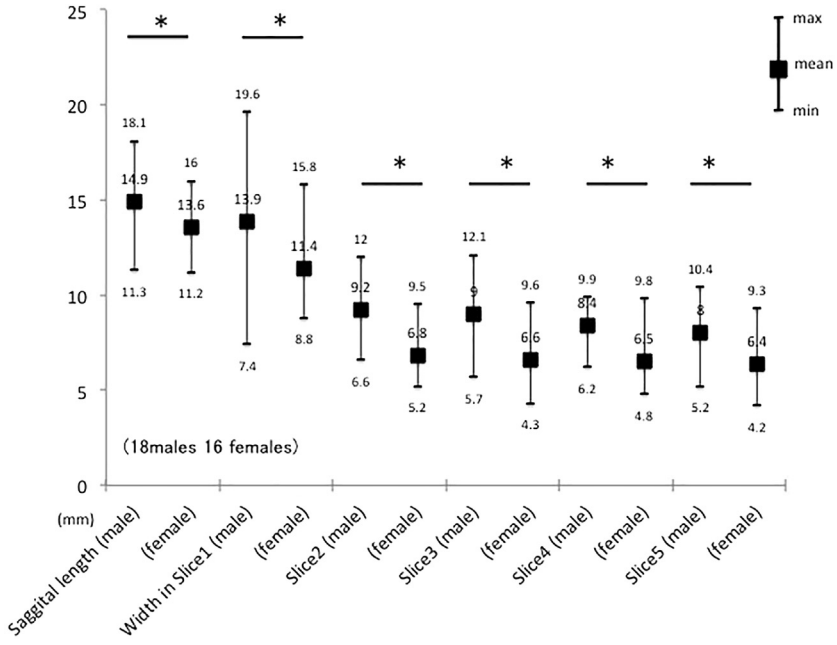

Figure 3. Size of the anterior cruciate ligament tibial insertion in male and female participants (*$P < 0.05$).

Ideal and accurate creation of the tibial tunnel is critical, while anterior positioning of the tibial tunnel brings better postoperative anterior knee stability [18–20]. The preoperative planning tailored to the individual bony landmarks might be useful not only for ideal anatomical ACL reconstruction but also for avoiding damage to the AHLM tibial insertion. Therefore, the tunnel aperture should be close to the MIR, and adjusted to the individual size of the ACL tibial insertion. Considering the width of the ACL tibial insertion is five or six millimeters for females (Figure 3), a single tunnel procedure may inevitably exceed this size limit. Therefore, a double/triple round tunnel or single rectangular tunnel technique might be considered, especially in female patients (Figure 3; Supplementary data S5) [21–26].

We recognize that this study has limitations. First, the analysis was limited to 34 knees and only among the Asian population. Although the shape and size of the insertions varied among specimens, CIR adjacent to the 'boot-like' shape of the ACL was clearly observed in all 34 knees. Furthermore, this study clarified the shapes and positional relationships of ACL and AHLM tibial insertions. While precise fiber conditions of the ACL and AHLM could not be observed in the CT images, characteristic bony landmarks and the positional relationship between ACL and AHLM tibial insertion, based on histologic evaluation, were precisely identified in 3D-CT and multiplanar reformation CT images.

5. Conclusion

The CIR lengthwise bisects the slope of MIR between the ACL and AHLM tibial insertions in healthy, young knees. The bony landmarks showed the boot-like shape of the ACL tibial insertion around the rectangular shape of AHLM tibial insertion, and the width of the insertion was proportional to individual body size. To minimize iatrogenic damage to the AHLM tibial insertion, this study may provide useful information for individual anatomical tibial tunnel creation with high accuracy.

Supplementary data to this article can be found online at https://doi.org/10.1016/j.knee.2019.04.009.

Conflict of interest

No benefits in any form have been received or will be received from a commercial party related directly or indirectly to the subject of this article. None of the authors have any conflicting interests related to the outcomes of this study.

References

[1] Watson JN, Wilson KJ, LaPrade CM, Kennedy NI, Campbell KJ, Hutchinson MR, et al. Iatrogenic injury of the anterior meniscal root attachments following anterior cruciate ligament reconstruction tunnel reaming. Knee Surg Sports Traumatol Arthrosc 2015;23:2360–6.
[2] LaPrade CM, Smith SD, Rasmussen MT, Hamming MG, Wijdicks CA, Engebretsen L, et al. Consequences of tibial tunnel reaming on the meniscal roots during cruciate ligament reconstruction in a cadaveric model, part 1: the anterior cruciate ligament. Am J Sports Med 2015;43:200–6.
[3] LaPrade CM, Ellman MB, Rasmussen MT, James EW, Wijdicks CA, Engebretsen L, et al. Anatomy of the anterior root attachments of the medial and lateral menisci: a quantitative analysis. Am J Sports Med 2014;42:2386–92.
[4] Jacobsen K. Area intercondylaris tibiae: osseous surface structure and its relation to soft tissue structures and applications to radiography. J Anat 1974;117:605–18.

[5] Berg EE. Parsons' knob (tuberculum intercondylare tertium). A guide to tibial anterior cruciate ligament insertion. Clin Orthop Relat Res 1993:229–31.
[6] Kusano M, Yonetani Y, Mae T, Nakata K, Yoshikawa H, Shino K. Tibial insertions of the anterior cruciate ligament and the anterior horn of the lateral meniscus: a histological and computed tomographic study. Knee 2017;24:782–91.
[7] Tanaka Y, Shiozaki Y, Yonetani Y, Kanamoto T, Tsujii A, Horibe S. MRI analysis of the attachment of the anteromedial and posterolateral bundles of anterior cruciate ligament using coronal oblique images. Knee Surg Sports Traumatol Arthrosc 2011;19(Suppl. 1):S54–9.
[8] Tensho K, Shimodaira H, Aoki T, Narita N, Kato H, Kakegawa A, et al. Bony landmarks of the anterior cruciate ligament tibial footprint: a detailed analysis comparing 3-dimensional computed tomography images to visual and histological evaluations. Am J Sports Med 2014;42:1433–40.
[9] Purnell ML, Larson AI, Clancy W. Anterior cruciate ligament insertions on the tibia and femur and their relationships to critical bony landmarks using high-resolution volume-rendering computed tomography. Am J Sports Med 2008;36:2083–90.
[10] Tensho K. Tibial insertion of the ACL: 3D-CT images, macroscopic, and microscopic findings. In: Mitsuo Ochi KS, Yasuda Kazunori, Kurosaka Masahiro, Yasukazu Yonetani, editors. ACL injury and its treatment. Japan: Springer Japan; 2016. p. 39–50.
[11] Siebold R, Schuhmacher P, Fernandez F, Smigielski R, Fink C, Brehmer A, et al. Flat midsubstance of the anterior cruciate ligament with tibial "C"-shaped insertion. Knee Surg Sports Traumatol Arthrosc 2015;23:3136–42.
[12] Heming JF, Rand J, Steiner ME. Anatomical limitations of transtibial drilling in anterior cruciate ligament reconstruction. Am J Sports Med 2007;35:1708–15.
[13] Kopf S, Pombo MW, Szczodry M, Irrgang JJ, Fu FH. Size variability of the human anterior cruciate ligament insertions. Am J Sports Med 2011;39:108–13.
[14] Tallay A, Lim MH, Bartlett J. Anatomical study of the human anterior cruciate ligament stump's tibial insertion footprint. Knee Surg Sports Traumatol Arthrosc 2008;16:741–6.
[15] Ferretti M, Doca D, Ingham SM, Cohen M, Fu FH. Bony and soft tissue landmarks of the ACL tibial insertion: an anatomical study. Knee Surg Sports Traumatol Arthrosc 2012;20:62–8.
[16] Tashiro Y, Lucidi GA, Gale T, Nagai K, Herbst E, Irrgang JJ, et al. Anterior cruciate ligament tibial insertion is elliptical or triangular shaped in healthy young adults: high-resolution 3-T MRI analysis. Knee Surg Sports Traumatol Arthrosc 2018;26:485–90.
[17] Benjamin M, Moriggl B, Brenner E, Emery P, McGonagle D, Redman S. The "enthesis organ" concept: why enthesopathies may not present as focal insertional disorders. Arthritis Rheum 2004;50:3306–13.
[18] Hatayama K, Terauchi M, Saito K, Higuchi H, Yanagisawa S, Takagishi K. The importance of tibial tunnel placement in anatomic double-bundle anterior cruciate ligament reconstruction. Arthroscopy 2013;29:1072–8.
[19] Inderhaug E, Strand T, Fischer-Bredenbeck C, Solheim E. Effect of a too posterior placement of the tibial tunnel on the outcome 10–12 years after anterior cruciate ligament reconstruction using the 70-degree tibial guide. Knee Surg Sports Traumatol Arthrosc 2014;22:1182–9.
[20] Zampeli F, Ntoulia A, Giotis D, Tsiaras VA, Argyropoulou M, Pappas E, et al. Correlation between anterior cruciate ligament graft obliquity and tibial rotation during dynamic pivoting activities in patients with anatomic anterior cruciate ligament reconstruction: an in vivo examination. Arthroscopy 2012;28:234–46.
[21] Otsubo H, Shino K, Nakamura N, Nakata K, Nakagawa S, Koyanagi M. Arthroscopic evaluation of ACL grafts reconstructed with the anatomical two-bundle technique using hamstring tendon autograft. Knee Surg Sports Traumatol Arthrosc 2007;15:720–8.
[22] Toritsuka Y, Amano H, Kuwano M, Iwai T, Mae T, Ohzono K, et al. Outcome of double-bundle ACL reconstruction using hamstring tendons. Knee Surg Sports Traumatol Arthrosc 2009;17:456–63.
[23] Shino K, Mae T, Tachibana Y. Anatomic ACL reconstruction: rectangular tunnel/bone–patellar tendon–bone or triple-bundle/semitendinosus tendon grafting. J Orthop Sci 2015;20:457–68.
[24] Tanaka Y, Shino K, Horibe S, Nakamura N, Nakagawa S, Mae T, et al. Triple-bundle ACL grafts evaluated by second-look arthroscopy. Knee Surg Sports Traumatol Arthrosc 2012;20:95–101.
[25] Shino K, Nakata K, Nakamura N, Toritsuka Y, Nakagawa S, Horibe S. Anatomically oriented anterior cruciate ligament reconstruction with a bone–patellar tendon–bone graft via rectangular socket and tunnel: a snug-fit and impingement-free grafting technique. Arthroscopy 2005;21:1402.
[26] Shino K, Nakata K, Nakamura N, Toritsuka Y, Horibe S, Nakagawa S, et al. Rectangular tunnel double-bundle anterior cruciate ligament reconstruction with bone–patellar tendon–bone graft to mimic natural fiber arrangement. Arthroscopy 2008;24:1178–83.